Pattern Recognition 45 (2012) 2769–2779

Contents lists available at SciVerse ScienceDirect

Pattern Recognition

journal homepage: www.elsevier.com/locate/pr

A local region-based Chan–Vese model for image segmentation

Shigang Liu [a,b], Yali Peng [a,*]

[a] School of Computer Science, Shaanxi Normal University, Xi'an 710062, China
[b] School of Electronics and Information Engineering, Xi'an Jiaotong University, Xi'an 710049, China

ARTICLE INFO

Article history:
Received 16 March 2011
Received in revised form
18 August 2011
Accepted 26 November 2011
Available online 10 January 2012

Keywords:
Active contour model
Image segmentation
Level set

ABSTRACT

In this paper, a new region-based active contour model, namely local region-based Chan–Vese (LRCV) model, is proposed for image segmentation. By considering the image local characteristics, the proposed model can effectively and efficiently segment images with intensity inhomogeneity. To reduce the dependency on manual initialization in many active contour models and for an automatic segmentation, a degraded CV model is proposed, whose segmentation result can be taken as the initial contour of the LRCV model. In addition, we regularize the level set function by using Gaussian filtering to keep it smooth in the evolution process. Experimental results on synthetic and real images show the advantages of our method in terms of both effectiveness and robustness. Compared with the well-know local binary fitting (LBF) model, our method is much more computationally efficient and much less sensitive to the initial contour.

1. Introduction

Image segmentation is the process of dividing images into meaningful subsets that correspond to surfaces or objects. It is a fundamental problem in the field of computer vision, because recognition and reconstruction often rely on this information [1,2]. To solve the problem, many researchers have done great efforts and proposed a wide variety of methods for image segmentation [3–5].

The active contour model (ACM) that is proposed by Kass et al. is one of the most successful models for image segmentation [6]. The basic idea of ACM is to evolve a curve to extract the desired object based on an energy-minimizing method. An advantage of ACM for image segmentation is that it partitions an image into sub-regions with closed and smooth boundaries. In early works the explicit snake model with a standard parametric curve representation was used [6,7]. However, it cannot conveniently deal with topological changes like the merging and splitting of the evolving curve. To over this drawback, many methods have been proposed, in which the most important and successful one is the PDE-based level set method introduced by Osher and Sethian [8]. It generalizes the Euler–Lagrange equation and evolves the interface which is represented implicitly as the zero level set of a function. An outstanding characteristic of level set methods is that contours can split or merge as the topology of the level set function changes. Therefore, the level set methods can detect more than one boundary simultaneously, and multiple initial contours can be placed. This flexibility and convenience provide a means for an automatic segmentation by using a predefined set of initial contours.

Without loss of generality, most of the ACMs studied under the level set framework can be categorized into two types: edge-based [8–10] and region-based [11–18] ones. The edge-based models utilize image gradient to construct force to direct the contours toward the boundaries of desired objects. These models are not only very sensitive to the noise, but also difficult to detect the weak boundaries. Moreover, the segmentation result is highly dependent on the initial contour placement. The region-based models utilize the image statistical information to construct constraints, which have many advantages of region-based approaches when compared with edge-based methods. First, they do not depend on the image gradient, and can satisfactorily segment the objects with weak boundaries. Second, by utilizing the global region information, they are generally robust to the noise.

The Mumford–Shah model, as a general image segmentation model, is firstly proposed by Mumford and Shah [12]. In this model, the image is decomposed into some regions that each region is approximated by a smooth function. The optimal partition of the image can be derived by minimizing the Mumford–Shah functional. However, the functional is non-convexity in generality, which make it difficult to be minimized.

One of the most popular region-based models is the Chan–Vese (CV) model [14], which is based on a simplified Mumford–Shah functional for segmentation. The CV model has been successfully applied for images with two regions which have a distinct mean of pixel intensity. But, in the CV model, the image intensities are assumed to be statistically homogeneous in each

* Corresponding author.
E-mail address: pengylxa@gmail.com (Y. Peng).

0031-3203/$ - see front matter © 2012 Elsevier Ltd. All rights reserved.
doi:10.1016/j.patcog.2011.11.019

region. However, the assumption does not hold for some general images, which limits its applications.

To solve the limitations of the CV model, Vese and Chan [15] and Tsai et al. [16] proposed two similar region-based active contour models by minimizing Mumford–Shah functional [12]. These models, widely known as piecewise smooth (PS) models, are based on a piecewise smooth description of the images. The PS models have exhibited certain capability of handling intensity inhomogeneity. However, the computational cost of the PS models is rather expensive due to the complicated procedures involved.

Recently, to solve the problem caused by intensity inhomogeneity, Li et al. proposed a local binary fitting (LBF) model [19]. Because of using local region information, specifically local intensity mean, the LBF model can cope with intensity inhomogeneity. Some related methods were recently proposed in [18,20] which have similar capability of handling intensity inhomogeneity as the LBF model. However, to some extent these methods are still sensitive to initial contour, which holds back their practical applications.

To improve the robustness to initialization, Wang et al. considered to combine the local intensity information and the global intensity information [21,22]. When the contour is far away from object boundaries, the force from the global intensity information is dominant and has large capture range. When the contour is close to the object boundaries, the force from the local intensity information becomes dominant, which attracts the contour toward and finally stops the contour at object boundaries. The technique of using global image information can improve the robustness to the initialization of contours. However, when the contour is close to the object boundaries, the interference from the global intensity force will result in the deviation of contour from the real object boundary.

In this paper, a new region-based active contour model, named local region-based Chan–Vese (LRCV) model, for image segmentation is proposed. By introducing the local image information into the proposed model, the images with intensity inhomogeneity can be effectively segmented. At the same time, to avoid the manually initialization, a degraded CV model is presented whose segmentation result is taken as the initial contour of the LRCV model. In addition, we use the Gaussian filtering to regularize our level set function, which keeps the level set function smooth. Experimental results on some synthetic and real images show the advantages of our method in terms of efficiency and robustness. Moreover, comparisons with the well-know local binary fitting (LBF) model also show that our method is more computationally efficient and robust to the location of initial contour.

The rest of this paper is organized as follows. In Section 2, we review some well-known region-based models and their limitations. The LRCV model is proposed in Section 3. The degraded CV model is introduced in Section 4. The implementation and results are given in Section 5. This paper is summarized in Section 6.

2. The review and discussion of related works

2.1. The Mumford–Shah model

The idea of Mumford–Shah function for image segmentation is to find an optimal contour C that partitions the image domain into disjoint sub-regions, and an optimal piecewise smooth function $u(x)$ that fits the original image $I(x)$ within each of the sub-regions. This can be formulated by minimizing the following energy functional:

$$E^{MS}(u,C)=\lambda\int_{\Omega}(I(x)-u(x))^2dx+\nu\int_{\Omega\setminus C}|\nabla u|^2dx+\mu\,\mathrm{Length}(C) \tag{1}$$

where C is a smooth and closed curve, $I(x)$ is the observed image data, $u(x)$ represents the piecewise smooth approximation to with discontinuities only along C, and Ω denotes the image domain. The parameters λ, ν and μ are positive constants. Usually, the first term in Eq. (1) is called the data fidelity term, which is taken as the measurement of $u(x)$; the second term is called the smoothness term, which is the prior model of $u(x)$given C; and the third term is called the prior model of C which penalizes excessive arc length. With these terms, the Mumford–Shah function based image segmentation can be performed by minimizing the energy functional over all the contours that fit $u(x)$. However, due to different nature of the two unknowns: the contour C and the function $u(x)$, and the non-convexity of the function as well, it is not easy to find the optimal solution to the above energy functional. For practical applications, many works [14,18–20] have been reported to simplify or modify the above Mumford–Shah functional, including the several well known approaches reviewed below.

2.2. The Chan–Vese (CV) model

Based on the special case of Mumford–Shah problem where the image $I(x)$ in the Eq. (1) is a piecewise constant function, Chan and Vese proposed an active contour approach for 2-phase image segmentation [14]. The basic idea is to look for a particular partition of a given image $I(x)$ into two regions, one representing the objects to be detected and the other representing the background. For a given image $I(x)$ on the image domain Ω, they proposed to minimize the following energy function:

$$E^{CV}(c_1,c_2,C)=\lambda_1\int_{in(C)}(I(x)-c_1)^2dx+\lambda_2\int_{out(C)}(I(x)-c_2)^2dx \tag{2}$$

where C represents the curve, the constants c_1 and c_2 denote the average intensities inside and outside the curve, respectively, and the coefficients λ_1 and λ_2 are fixed parameters.

In the Chan–Vese model, they also have a regularizing term, such as the length of C and the area inside C to control the smoothness of the boundary. Therefore, the energy $E^{CV}(c_1,c_2,C)$ is defined by

$$\begin{aligned}E^{CV}(c_1,c_2,C)=&\lambda_1\int_{in(C)}(I(x)-c_1)^2dx+\lambda_2\int_{out(C)}(I(x)-c_2)^2dx\\&+\mu\,\mathrm{Length}(C)+\upsilon\,\mathrm{Area}(in(C))\end{aligned} \tag{3}$$

Using the level set to represent C, that is, C is the zero level set of a Lipschitz function $\phi(x)$, we can replace the unknown variable C by the unknown variable $\phi(x)$, and the energy function $E^{CV}(c_1,c_2,C)$ can be written as

$$\begin{aligned}E^{CV}(c_1,c_2,\phi)=&\lambda_1\int_{\Omega}(I(x)-c_1)^2H(\phi(x))dx+\lambda_2\int_{\Omega}(I(x)-c_2)^2(1-H(\phi(x)))dx\\&+\mu\int_{\Omega}\delta(\phi(x))|\nabla\phi(x)|dx+\upsilon\int_{\Omega}H(\phi(x))dx\end{aligned} \tag{4}$$

where $H(\phi)$ and $\delta(\phi)$ are Heaviside function and Dirac function, respectively. Generally, the regularized versions are selected as

$$\begin{cases}H_\varepsilon(z)=\frac{1}{2}\left(1+\frac{2}{\pi}\arctan\left(\frac{z}{\varepsilon}\right)\right)\\ \delta_\varepsilon(z)=\frac{1}{\pi}\frac{\varepsilon}{\varepsilon^2+z^2}\end{cases}\quad z\in R \tag{5}$$

Keeping $\phi(x)$ fixed and minimizing the energy $E^{CV}(c_1,c_2,\phi)$ with respect to the constants c_1 and c_2, we have

$$\begin{cases}c_1(\phi)=\frac{\int_{\Omega}I(x)H(\phi(x))dx}{\int_{\Omega}H(\phi(x))dx}\\ c_2(\phi)=\frac{\int_{\Omega}I(x)(1-H(\phi(x)))dx}{\int_{\Omega}(1-H(\phi(x)))dx}\end{cases} \tag{6}$$

In fact, c_1 and c_2 are given by

$$\begin{cases} c_1(\phi) = \text{average}(I) & in\{\phi \geq 0\} \\ c_2(\phi) = \text{average}(I) & in\{\phi < 0\} \end{cases} \tag{7}$$

At the same time, keeping c_1 and c_2 fixed, we minimize $E^{CV}(c_1,c_2,\phi)$ with respect to $\phi(x)$, and deduce the associated Euler–Lagrange equation for $\phi(x)$. Parameterizing the descent direction by an artificial time t, we can obtain the corresponding variational level set formulation as follows:

$$\frac{\partial \phi(x,t)}{\partial t} = \delta(\phi)\left[-\lambda_1(I(x)-c_1)^2 + \lambda_2(I(x)-c_2)^2 + \mu \,\text{div}\left(\frac{\nabla\phi}{|\nabla\phi|}\right) - \upsilon\right] \tag{8}$$

The CV model has good performance in image segmentation due to its ability of obtaining a larger convergence range and being less sensitive to the initialization. However, the CV model is only adapted for 2-phase image. If the intensities with inside C or outside C are not homogeneous, the constants c_1 and c_2 will not be accurate. As a consequence, the CV model generally fails to segment images with intensity inhomogeneity. Similarly, more general piecewise constant models in a multiphase level set framework are not good at such images either [15].

2.3. Local binary fitting active contour model (LBF)

To overcome the difficulty caused by intensity inhomogeneities, Li et al. proposed the local binary fitting (LBF) model [19,20], which can utilize the local intensity information. In the LBF model, two spatially varying fitting functions $f_1(x)$ and $f_2(x)$ are introduce to approximate the local intensities on the two sides of the contour, and for a given point $x \in \Omega$, the local intensity fitting energy is defined by

$$E_x(C,f_1,f_2) = \lambda_1 \int_{in(C)} g(x-y)(I(v)-f_1(x))^2 dy + \lambda_2 \int_{out(C)} g(x-y)(I(y)-f_2(x))^2 dy \tag{9}$$

where λ_1 and λ_2 are positive constants, $g(y)$ is a Gaussian kernel function, and $f_1(x)$ and $f_2(x)$ are two values that approximate image intensities inside and outside contour C, respectively.

The above local fitting energy $E_x(C,f_1(x),f_2(x))$ is defined for a center point x. For all the center point x in the image domain Ω, the energy function can be defined by

$$E^{LBF}(C,f_1(x),f_2(x)) = \int_{\Omega} E_x(C,f_1(x),f_2(x))dx \tag{10}$$

Inserting Eq. (9) into Eq. (10), and using the level set function ϕ to represent the contour C, we have

$$\begin{aligned} E^{LBF}(\phi,f_1(x),f_2(x)) = {} & \lambda_1 \int_{\Omega}\left[\int_{\Omega} g(x-y)(I(y)-f_1(x))^2 H(\phi(y))dy\right]dx \\ & + \lambda_2 \int_{\Omega}\left[\int_{\Omega} g(x-y)(I(y)-f_2(x))^2 (1-H(\phi(y)))dy\right]dx \end{aligned} \tag{11}$$

For more accurate computation involving the level set function and its evolution, we regularize the level set function by penalizing its deviation from a signed distance function. At the same time, we also have a regularizing the length of C to control the smoothness of the boundary. The two terms can be characterized by the following energy function:

$$E^R(\phi) = \mu \int_{\Omega} \delta(\phi(x))|\nabla\phi(x)|dx + \nu \int_{\Omega} \frac{1}{2}(|\nabla\phi(x)|-1)dx \tag{12}$$

Therefore, we can define the following energy function:

$$E^{LBF}_{all}(\phi,f_1(x),f_2(x)) = E^{LBF}(\phi,f_1(x),f_2(x)) + E^R(\phi) \tag{13}$$

Keeping level set function ϕ fixed, and minimizing the function $E^{LBF}_{all}(\phi,f_1(x),f_2(x))$ in Eq. (13) with respect to the function $f_1(x)$ and $f_2(x)$, we have

$$\begin{cases} f_1(x) = \frac{g(x)[H(\phi(x))I(x)]}{g(x)H(\phi(x))} \\ f_2(x) = \frac{g(x)[1-H(\phi(x))I(x)]}{g(x)[1-H(\phi(x))]} \end{cases} \tag{14}$$

Fixing $f_1(x)$ and $f_2(x)$, we minimize the energy function $E^{LBF}_{all}(\phi,f_1(x),f_2(x))$ with respect to ϕ, and have the gradient descent flow

$$\frac{\partial \phi}{\partial t} = \delta(\phi)\left(\mu \,\text{div}\left(\frac{\nabla\phi}{|\nabla\phi|}\right) - \lambda_1 e_1 + \lambda_2 e_2\right) + \nu\left(\nabla^2\phi - \text{div}\left(\frac{\nabla\phi}{|\nabla\phi|}\right)\right) \tag{15}$$

where e_1 and e_2 are the functions as below

$$\begin{cases} e_1 = \int_{\Omega} g(y-x)|I(x)-f_1(y)|^2 dy \\ e_2 = \int_{\Omega} g(y-x)|I(x)-f_2(y)|^2 dy \end{cases} \tag{16}$$

Because of using local region information, specifically local intensity mean, the LBF model is able to provide desirable segmentation results even in the presence of intensity inhomogeneity. At the same time, the time-consuming re-initialization step widely adopted in traditional level set methods is avoided by introducing a new penalizing energy to the regularization term. As a result, the time-consumption is heavily decreased. However, the computational cost is still very high, which is pointed out by Zhang et al. [18]. In addition, the LBF model is sensitive to initialization to some extent [21], which limits its practical applications.

2.4. The local Chan–Vese (LCV) model

Wang et al. proposed a local Chan–Vese (LCV) model which can utilize both global image information and local image information for image segmentation [22]. For the LCV model, the energy functional which consists of three parts: global term E^G, local term E^L and regularization term E^R is defined as following:

$$E^{LCV} = \alpha E^G + \beta E^L + E^R \tag{17}$$

where α and β are fixed constants, the global term E^G is from the CV model and the local term E^L is defined by as below

$$E^L(d_1,d_2,C) = \int_{in(C)} (g_k I(x) - I(x) - d_1)^2 dx + \int_{out(C)} (g_k I(x) - I(x) - d_2)^2 dx \tag{18}$$

where g_k is an averaging filter with $k \times k$ size, d_1 and d_2 are the intensity averages of the difference image $g_k I(x) - I(x)$ inside C and outside C, respectively.

Representing the contour with zero level set and minimizing E^{LCV}, the following variational formulations can be obtained:

$$\begin{cases} c_1 = \frac{\int_{\Omega} I(x)H(\phi(x))dx}{\int_{\Omega} H(\phi(x))dx} \\ c_2 = \frac{\int_{\Omega} I(x)(1-H(\phi(x)))dx}{\int_{\Omega}(1-H(\phi(x)))dx} \end{cases} \tag{19}$$

$$\begin{cases} d_1 = \frac{\int_{\Omega}(g_k I(x) - I(x))H(\phi(x))dx}{\int_{\Omega} H(\phi(x))dx} \\ d_2 = \frac{\int_{\Omega}(g_k I(x) - I(x))(1-H(\phi(x)))dx}{\int_{\Omega}(1-H(\phi(x)))dx} \end{cases} \tag{20}$$

$$\begin{aligned} \frac{\partial \phi}{\partial t} = {} & \delta(\phi)(-\alpha(I-c_1)^2 + \alpha(I-c_2)^2) + \delta(\phi)(-\beta(g_k I - I - d_1)^2 \\ & + \beta(g_k I - I - d_2)^2) + \mu\delta(\phi)\text{div}\left(\frac{\nabla\phi}{|\nabla\phi|}\right) + \nabla^2\phi - \text{div}\left(\frac{\nabla\phi}{|\nabla\phi|}\right) \end{aligned} \tag{21}$$

To easily analyze the local term of the LCV model, we discard the global term and the regularization term in the energy functional Eq. (17), and let

$$I'(x) = g_k I(x) - I(x) \tag{22}$$

Inserting Eq. (22) into Eqs. (18), (20) and (21), we have

$$E^L(d_1,d_2,C) = \int_{in(C)} (I'(x)-d_1)^2 dx + \int_{out(C)} (I'(x)-d_2)^2 dx \tag{23}$$

$$\begin{cases} d_1(\phi) = \frac{\int_\Omega I'(x)H(\phi(x)dx}{\int_\Omega H(\phi(x)dx} \\ d_2(\phi) = \frac{\int_\Omega I(x)(1-H(\phi(x))dx}{\int_\Omega (1-H(\phi(x)))dx} \end{cases} \tag{24}$$

$$\frac{\partial \phi}{\partial t} = \delta(\phi)(-\beta(I'(x)-d_1)^2 + \beta(I'(x)-d_2)^2) \tag{25}$$

Comparing Eqs. (24) and (19), Eq. (25) and the first term in Eq. (21), respectively, we can find the local term of LCV model is same as the global term except that the original image $I(x)$ is substituted by $I'(x)$. The transformation from $I(x)$ to $I'(x)$ defined by Eq. (22) is a high-pass filter which can result in the appearance of the double contours. At the same time, the edges of the transformed image $I'(x)$ are blurred.

Form above analysis, the local term E^L of the LCV model can be regarded as the energy function that the CV model acts on the image $I'(x)$ transformed from $I(x)$. So, to some extent, the LCV model can be taken as the CV model acting on the image which is a combination of the original image $I(x)$ with its transformed $I'(x)$. As is well known to all, the CV model is only suitable for the image with piecewise constant intensities or approximately piecewise constant intensities. However, it is impossible for the transformation $I'(x)$ defined by Eq. (22) to become an image with piecewise constant intensities or approximately piecewise constant intensities. So, it is difficult to obtain right segmentation result from the LCV model.

The technique of using global image information can improve the robustness to initialization of contours. However, when the contour is close to object boundaries, the interference from the global intensity force will result to the deviation of contour from the real object boundary. At the same time, the double contours will appear and the edge position becomes blurred and inaccurate in the LCV model. Furthermore, the LCV model can be taken as the CV model acting on the image which is a combination of the original image and its transformed. To some extend, the LCV model is also a CV model. So, it is difficult for the LCV model to satisfactorily segment the image with intensity inhomogeneity.

3. Local region-based Chan–Vese (LRCV) model

In this section, we present and discuss in detail the proposed local region-based Chan–Vese (LRCV) model. In the CV model, the parameters c_1 and c_2 are constants that represent respectively the average intensities inside and outside the curve. For a point $x \in R^2$, its intensity can be approximated by a weighted average of the image intensity $I(y)$ where y is the neighborhood of x. Therefore, we can replace the two constants c_1 and c_2 of the CV model by the following functions which are spatially varying.

$$\begin{cases} c_1(x) = \frac{\int_\Omega g_k(x-y)(I(y)H(\phi(y)))dy}{\int_\Omega g_k(x-y)H(\phi(y))dy} \\ c_2(x) = \frac{\int_\Omega g_k(x-y)(I(y)(1-H(\phi(y))))dy}{\int_\Omega g_k(x-y)(1-H(\phi(y)))dy} \end{cases} \tag{26}$$

where g_k is a Gaussian kernel function.

From Eq. (26), we can see that $g_k(x-y)$ can be taken as the weight assigned to each intensity $I(y)$ at y. Due to the localization property of the kernel function g_k, the contribution of the

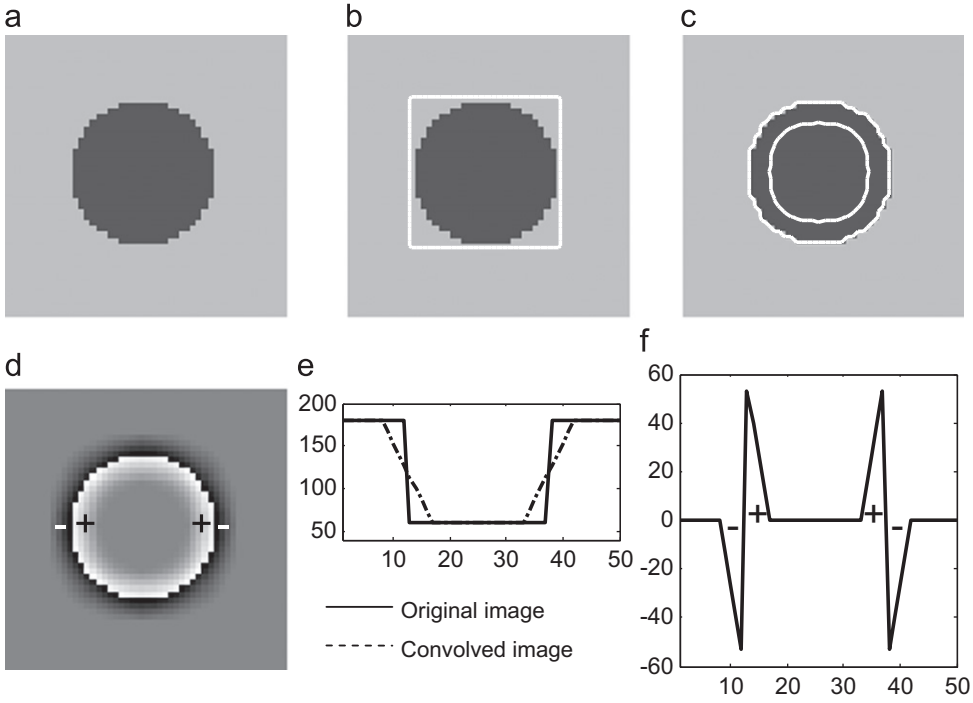

Fig. 1. The segmentation of the LCV model. (a) Original image with size 50×50; (b) initial contour; (c) final segmentation result with kernel size 9×9; (d) transformed image. (e) The intensity value in the middle row of the original image (solid line) and its corresponding convolved image (dashed line). (f) The intensity value in the middle row of transformed image. '+' and '−' are the signs of intensity value.

intensity $I(y)$ to $c_1(x)$ and $c_2(x)$ decreases and approaches to zero as the point y goes away from the center point x. Therefore, $c_1(x)$ and $c_2(x)$ are dominated by the intensities of the points in a neighborhood of the point x, which is similar to the LBF model. If g_k is an averaging filter and the size of its window is infinity, the function $c_1(x)$ and $c_2(x)$ become constants which represent the average intensities inside and outside the curve, respectively, and obviously the LRCV model degenerates to the CV model. In this sense, the CV model is a special case of the LRCV model.

Substituting Eq. (26) into Eq. (2), we can obtain the energy functional of the proposed model as follows:

$$E(c_1(x),c_2(x),C)=\lambda_1\int_{in(C)}(I(x)-c_1(x))^2dx+\lambda_2\int_{out(C)}(I(x)-c_2(x))^2dx \tag{27}$$

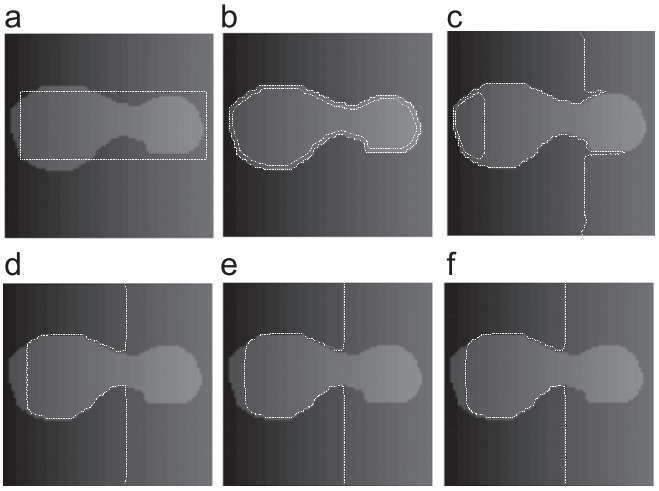

Fig. 2. Segmentation results by the LCV model. (a) Initial contour; (b), (c), (d), (e) and (f) are the segmentation results with ($\alpha=0$, $\beta=1$), ($\alpha=0.01$, $\beta=1$), ($\alpha=0.1$, $\beta=1$), ($\alpha=1$, $\beta=1$) and ($\alpha=1$, $\beta=0$), respectively.

Using the level set function ϕ to represent the contour C in the domain Ω, the energy functional can be rewritten as

$$E(c_1,c_2,\phi)=\lambda_1\int_{\Omega}(I(x)-c_1(x))^2H(\phi(x))dx+\lambda_2\int_{\Omega}(I(x)-c_2(x))^2(1-H(\phi(x)))dx \tag{28}$$

By keeping $c_1(x)$ and $c_2(x)$ fixed, we minimize the energy functional $E(c_1,c_2,\phi)$ with respect to ϕ to obtain the gradient descent flow as

$$\frac{\partial\phi(x,t)}{\partial t}=\delta(\phi)\left[-\lambda_1(I(x)-c_1(x))^2+\lambda_2(I(x)-c_2(x))^2\right] \tag{29}$$

Note that the above gradient descent flow is very similar to Eq. (8). c_1 and c_2 are constants in the CV model, while $c_1(x)$ and $c_2(x)$ are spatially varying in our model.

In the proposed LRCV model, the main computational cost comes from computing $c_1(x)$ and $c_2(x)$ in Eq. (26). At the first sight, there are four convolutions to compute $c_1(x)$ and $c_2(x)$. It can be noticed that the expression can be rewritten to the combination of the four convolutions $\int_\Omega g_k(x-y)dy$, $\int_\Omega g_k(x-y)I(y)dy$, $\int_\Omega g_k(x-y)H(\phi(y))dy$ and $\int_\Omega g_k(x-y)(I(y)H(\phi(y)))dy$, and the terms $\int_\Omega g_k(x-y)dy$ and $\int_\Omega g_k(x-y)I(y)dy$ do not depend on the evolution of level set function ϕ. The two convolutions $\int_\Omega g_k(x-y)dy$ and $\int_\Omega g_k(x-y)I(y)dy$ can be computed only once before the iterations. Therefore, there are only two convolutions $\int_\Omega g_k(x-y)H(\phi(y))dy$ and $\int_\Omega g_k(x-y)(I(y)H(\phi(y)))dy$ to be computed at each iteration. In comparison, there are at least four convolutions in the LBF model [20]. So, for each iteration, the computational cost of the LRCV model is about half that of the LBF model.

In the traditional level set methods [14–17], the level set function should be a signed distance function to its interface during the evolution to prevent the level set function ϕ from being too steep or flat. It is necessary to re-initialize the level set function to shape the degraded level set function. However, this process is very time-consuming. To solve this problem, Li et al. [10] proposed a variational formulation penalizing the deviation of the level set function from a sign distance function. This strategy reduces the computational cost to some extent. However, the method is sensitive to initialization [22].

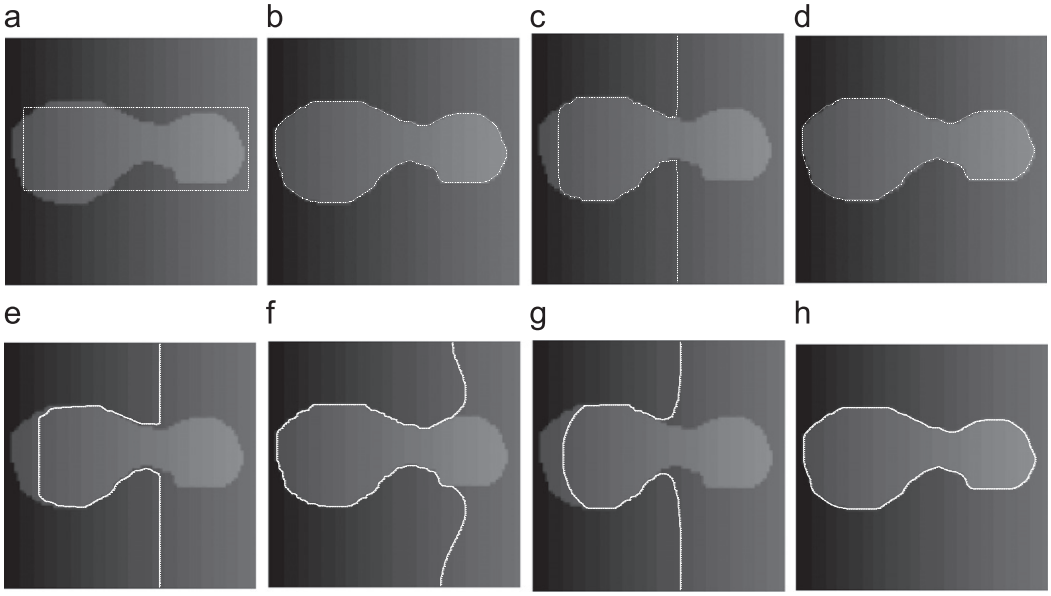

Fig. 3. Comparisons of the LBF model, the LCV model and the LRCV model on segmentation results. Row 1: the initial contours; Row 2: the initial contours from the degraded CV model. Column 1: initial contours; Column 2: segmentation results by the LBF model; Column 3: segmentation results by the LCV model; Column 4: segmentation results by the LRCV model.

In order to efficiently and robustly regularize the level set function, we can replace the regularization of the level set function ϕ by using a Gaussian filtering process, which is pointed out by Zhang et al. [18]. In the strategy, the standard deviation of the Gaussian filter can be used to control the regularization strength, as the parameter μ does in the LBF model. The smoothness regularization term is substituted by the following equation:

$$\phi^{n+1} = g_{\sqrt{\Delta t}}\phi^n \tag{30}$$

where Δt is time step-length and $g_{\sqrt{\Delta t}}$ is a Gaussian kernel with variance Δt.

The main steps of the algorithm can be summarized as:

Step 1: Initialize the level set function ϕ to be a binary function as following:

$$\phi(x,t=0) = \begin{cases} -\rho & x \in \Omega_0 - \partial\Omega_0 \\ 0 & x \in \partial\Omega_0 \\ \rho & x \in \Omega - \Omega_0 \end{cases} \tag{31}$$

where $\rho > 0$ is a constant, Ω_0 is a subset in the image domain and $\partial\Omega_0$ is the boundary of Ω_0.

Step 2: Compute $c_1(x)$ and $c_2(x)$ from Eq. (26).

Step 3: Evolve the level set function ϕ according to Eq. (29).

Step 4: Regularize the level set function by a Gaussian kernel as Eq. (30).

Step 5: Check whether the evolution is stationary. If not, return to *step* 2.

4. The degraded CV (DCV) model

In our model, if $c_1(x)$ and $c_2(x)$ degrade to constants, the proposed LRCV model becomes the CV model. Furthermore, let $\lambda_1 = \lambda_2 = \lambda$, then Eq. (29) becomes

$$\frac{\partial\phi(x,t)}{\partial t} = 2\delta(\phi)\lambda(c_1 - c_2)\left[I(x) - \frac{(c_1+c_2)}{2}\right] \tag{32}$$

During the level set evolution, the coefficient $2\lambda(c_1 - c_2)$ can be regarded as a constant. Therefore, we can omit the coefficient, and Eq. (32) becomes

$$\frac{\partial\phi(x,t)}{\partial t} = \delta(\phi)\left(I(x) - \frac{(c_1+c_2)}{2}\right) \tag{33}$$

Because the image $I(x)$ is independent of time t, Eq. 33 is an ordinary differential equation, which has many advantages over partial differential equations. As described above, we can substitute $\delta(\phi)$ by $|\nabla(\phi)|$ to enlarge the convergence range. Then, Eq. (33) becomes the Hamilton-Jacobi equation and the evolution speed term is $(I(x) - ((c_1+c_2)/2))$. When the speed term is negative, the curve evolves toward the normal direction. On the contrary, the curve evolves toward the opposite direction. Such a degraded CV model can segments efficiently the binary image and the convergence speed is very fast, which is similar to the one proposed by Zhang et al. [11]. Therefore, we can use this model to pre-segment the image and then take the segmentation curve as the initial contour of the LRBF model.

It is easy to initialize the level set function in the degraded CV model. Actually we can let the initialization of the level set function $\phi^0 = 0$ and then we have $H_\varepsilon(\phi^0) = 1/2$ from Eq. (5). From

Table 1
Comparison of the number of iterations and CPU time.

	The LBF model		The LCV model		The LRCV model	
	Iterations	CPU time(s)	Iterations	CPU time(s)	Iterations	CPU time(s)
Row 1	20	4.234	150	56.381	8	0.802
Row 2	100	48.980	700	237.401	50	3.067

Table 2
Comparison of the number of iterations and CPU time.

	The LBF model		The LCV model		The LRCV model	
	Iterations	CPU time(s)	Iterations	CPU time(s)	Iterations	CPU time(s)
Row 1	140	3.425	400	23.346	500	1.788
Row 2	20	0.509	1000	50.859	950	3.932

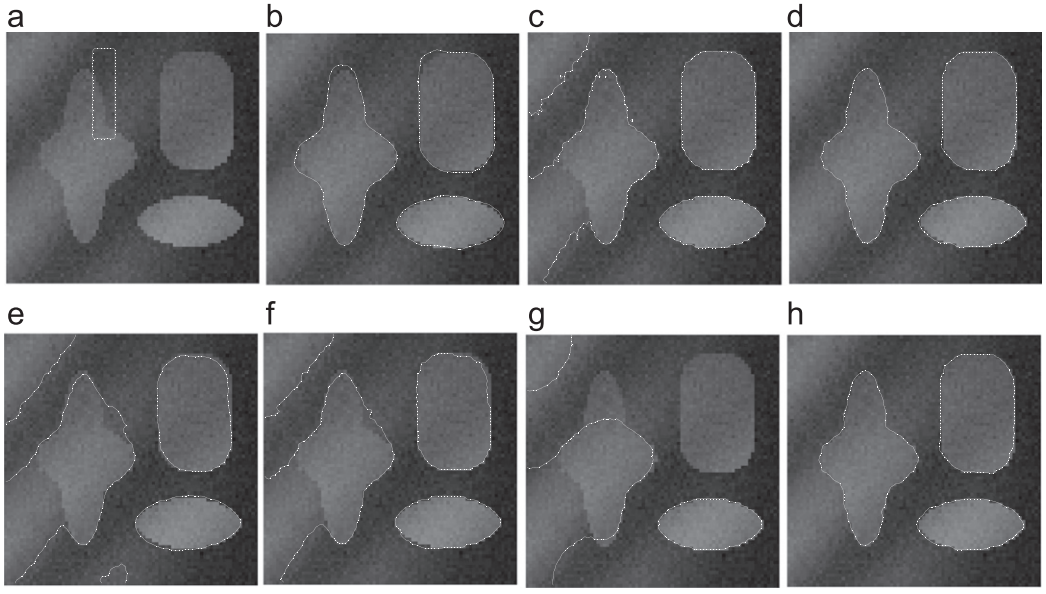

Fig. 4. Comparisons of the LBF model, the LCV model and the LRCV model on segmentation results. Row 1: the initial contours given in [23]; Row 2: the initial contours from the degraded CV model. Column 1: initial contours; Column 2: segmentation results by the LBF model; Column 3: segmentation results by the LCV model ($\alpha = 0.1$, $\beta = 1$, $\mu = 0.01 \times 255^2$); Column 4: segmentation results by the LRCV model.

Eq. (6), we can obtain

$$c_1(\phi^0) = c_2(\phi^0) = \text{average}(I) \tag{34}$$

After one iteration, the level set function $\phi(x,t)$ becomes

$$\phi^1 = \Delta t(I(x) - \text{average}(I)) \tag{35}$$

Because $I(x)$ is not a single value function, the level set function ϕ^1 has both minus and positive values from above expression. Therefore, the contour which is defined by zero level set function appears. From our experiments, we found that after only a few iterations, typically 3 or 4, the evolution of the contour stopped, so this procedure is very efficient, which cannot burden our LRCV method in terms of efficiency.

With the above procedures, the initialization of level set function in the degraded CV model can be completely automatic without any human interfaces. The segmentation result can then be taken as the initial contour for the evolution of the LRCV model.

5. Experiments

In this section, we evaluate and compare the proposed LRCV model with the LBF [19] and recently developed LCV [22] models

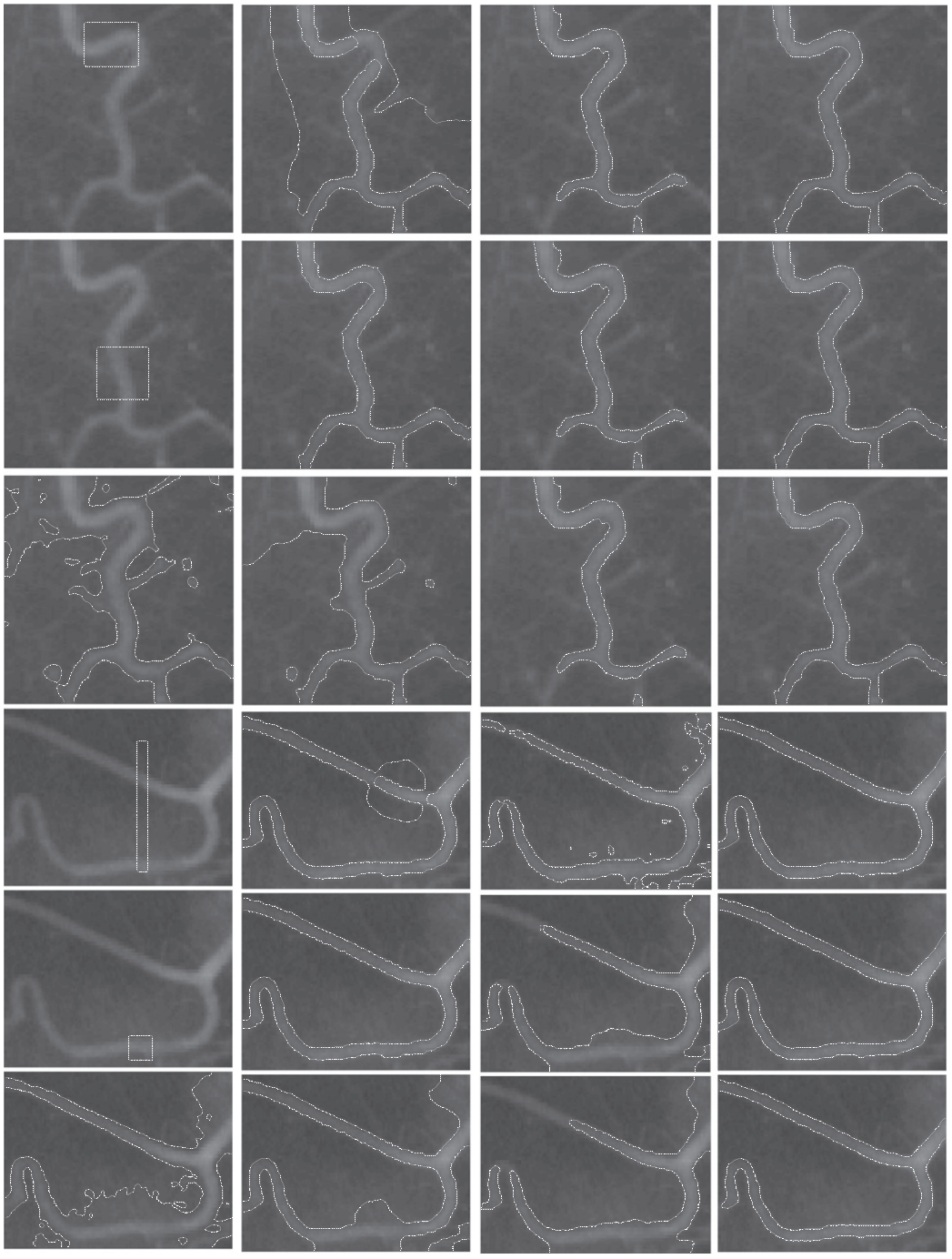

Fig. 5. Comparisons of the LBF model, the LCV model and the LRCV model on segmentation results. l. Rows 2 and 5: the initial contours given in [23]; Rows 3 and 6: the initial contours from the degraded CV model. Column 1: initial contours; Column 2: segmentation results by the LBF model; Column 3: segmentation results by the LCV model ($\alpha=0.1$, $\beta=1$, $\mu=0.001\times 255^2$); Column 4: segmentation results by the LRCV model.

using both synthetic and real images. All the experiments were conducted in Matlab 7.0 programming environment on a 1.6 GHz Intel Pentium IV personal computer.

Firstly, the LCV model is used to segment the synthetic image with size 50×50 in Fig. 1(a) which is typical example of image with piecewise-constant intensities. The intensity values of the background and the object are 180 and 60, respectively. To show the action of local term of the LCV model, we let $\alpha=0$, $\beta=1$ in Eq. (17), i.e., neglect the global term, and segment the image with the initial contour which is shown in Fig. 1(b). We set the kernel size 9×9 and obtain the segmentation results in Fig. 1(c).

From the segmentation result shown in Fig. 1(c), we can find that the double contours appear. Because the local term E^L of the LCV model in Eq. (17) is can be taken as the CV model that acts on the image $I'(x)$ transformed from $I(x)$ and the transformation defined by Eq. (22) is a high-pass filter which can result in the appearance of the double contours. In addition, the edges of the transformed image $I'(x)$ are blurred as shown in Fig. 1(d).

To further explain how the double contours are to appear, we extract the intensity value of the middle row from the original image and its corresponding convolved image which are denoted by the solid line and dashed line in Fig. 1(e), respectively. Fig. 1(f) shows the intensity value from the middle row of the transformed image, which also comes from the difference between the values denoted by the solid line and the dashed line in Fig. 1(e). In Fig. 1(d) and (f), '+' and '−' are the signs of intensity value. From Fig. 1(f), we can obviously observe the transformed image $I'(x)$ will cause the double contours to appear.

We test another synthetic image, in which the right part of background has higher intensities than the left part of object. Fig. 2 shows the results by the LCV model proposed by Wang et al. [22]. The size of the averaging convolution kernel was set as 9×9. Fig. 2(a) is initial contour. Fig. 2(b), (c), (d) (e) and (f) are the segmentation results with ($\alpha=0$, $\beta=1$), ($\alpha=0.01$, $\beta=1$), ($\alpha=0.1$, $\beta=1$), ($\alpha=1$, $\beta=1$) and ($\alpha=1$, $\beta=0$), respectively. Note that when $\alpha=1$ and $\beta=0$, the LCV model degrades to the CV model. The image characteristic which the part of the background has higher intensities than the part of the object makes it is impossible for the CV model to satisfactorily segment the image. When $\alpha=0$ and $\beta=1$, the global term from the CV model is discarded and the segmentation result is dominated by the local term and the regularization term. The double contours appear as shown in Fig. 2(b). When $\alpha=0.01$ and $\beta=1$, we can see from Fig. 2(c) that the global intensity fitting force and the local one interact with each other, which leads to inaccurate segmentation. The similar segmentation results can be observed in Fig. 2(d), (e) and (f) with ($\alpha=0.1$, $\beta=1$), ($\alpha=1$, $\beta=1$) and ($\alpha=1$, $\beta=0$), respectively. From Fig. 2(c) and (d), we can observe that although the coefficient α is small, the segmentation results are close to that by the CV model, which implies that the force from the global term is far more significant than the local term in the LCV model.

Let us then compare the segmentation results by the LBF model, the LCV model and the proposed LRCV model on the same image and they have the same initial contours shown in Fig. 3. In Fig. 3, Column 1 is the initial contours and Columns 2, 3 and 4 are segmentation results by the LBF model, the LCV model and the proposed LRCV model, respectively. From Column 3, we can observe that the right

Table 3
Comparison of the number of iterations and CPU time.

	The LBF model		The LCV model		The LRCV model	
	Iterations	CPU time(s)	Iterations time(s)	CPU time(s)	Iterations time(s)	CPU time(s)
Row 1	120	5.634	300	30.576	35	1.947
Row 2	100	4.923	280	23.647	40	0.586
Row 3	500	25.632	2000	150.341	40	2.283
Row 4	400	22.478	1200	90.692	30	1.719
Row 5	220	11.384	500	44.251	18	1.1936
Row 6	320	15.127	800	70.624	20	1.313

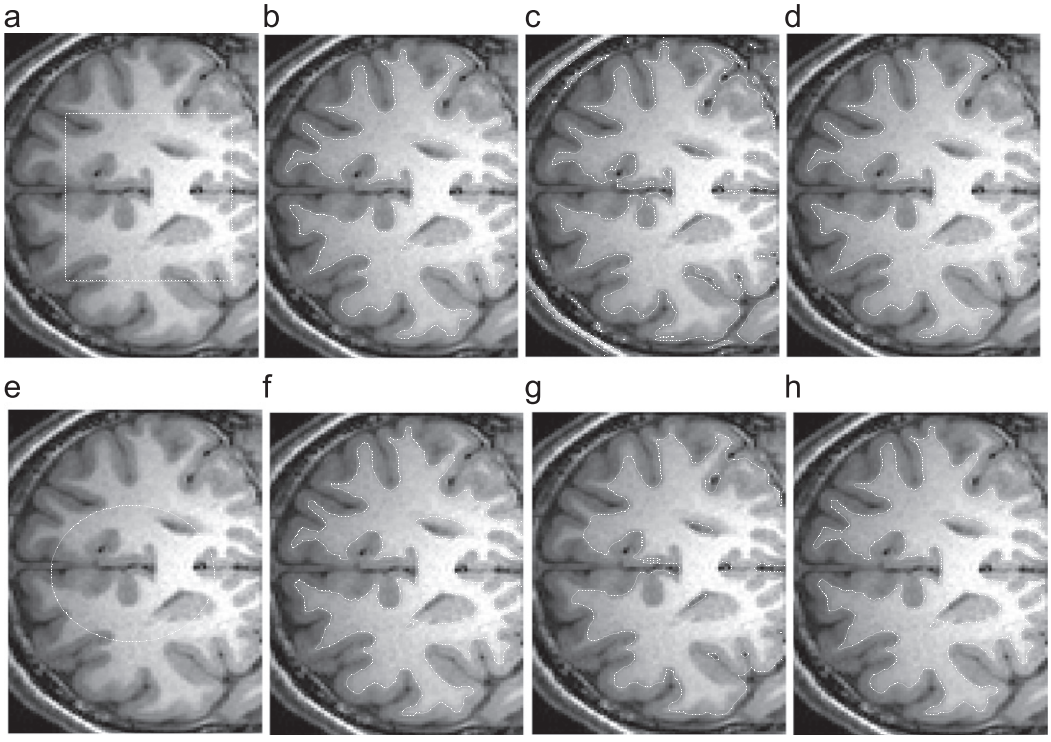

Fig. 6. The segmentation of a brain MR image by the LBF model, the LCV model and the LRCV model. Column 1: initial contours; Column 2: segmentation results by the LBF model; Column 3: segmentation results by the LCV model ($\alpha=0.1$, $\beta=1$, $\mu=0.001 \times 255^2$); Column 4: segmentation results by the LRCV model.

segmentation result cannot be obtained from the LCV model. Note that the parameters are set to ($\alpha=0.1$, $\beta=1$, $\mu=0.01\times 255^2$) which are from [22]. In Row 1, both the LBF model and the proposed LRCV model can satisfactorily segment the object. For the initial contour of Row 2 which is from the degraded CV model, we can observe from Fig. 3(f) and (h) that the LBF model fails to segment the object, while the right segmentation is obtained from the proposed LRCV model. Table 1 shows the number of iterations and CPU time of the three models.

From Table 1, we can observe that the LCV model has most iterations and CPU time among the three models and the LBF model has more than twice iterations and more than 5 times CPU time as much as the proposed LRCV model.

Let us use another synthetic image to compare the LBF model, the LCV model and the proposed LRCV model. The results are shown in Fig. 4. Column 3 shows that the LCV model fails to segment the object for both of the initial contours. In Row 1, the initial contour is set as the same as that in [23]. We can see that the same segmentation results are obtained by the LBF model and the proposed LRCV model, as shown in Fig. 4(b) and (d), while the LCV model fails to segment the object as shown in Fig. 4(c). For an automatic initialization, we use the segmentation result of the degraded CV model as the initial contour shown in Fig. 4(e). The results by the LBF model, the LCV model and the proposed LRCV model are shown in Fig. 4(f), (g) and (h), respectively. We can see that the LBF model and the LCV model fail to segment the object while the proposed LRCV model succeeds. Table 2 lists the number of iterations and CPU time of the three models. For both of the initial contours, the LCV model has most iterations and CPU time. What's more, the LCV model fails to segment the object. With the manually drawn contour in [23], although the LBF model has less iteration than the proposed LRCV model, it spends more CPU time than LRCV. With the contour generated from the degraded CV model, the LBF model has less iterations and CPU time than our model. But it fails to satisfactorily segment the object in this experiment.

To further evaluate the performance of the proposed method, we apply the LBF model, the LCV model and the proposed LRCV model to real blood vessel images which have intensity inhomogeneity. Refer to Fig. 5, the first column shows various initial contours; the second, third and fourth column are the segmentation results by the LBF model, the LCV model and the LRCV model, respectively. The initial contours in Rows 3 and 6 are generated by the degraded CV model. For both of the initial contours, the right segmentation result cannot be obtained from the LCV model. Note that in LCV model the parameters are set to $\alpha=0.1$, $\beta=1$, $\mu=0.001\times 255^2$ which are from [22]. For some initial contours, as shown in Rows 1, 3 and 4, the LBF model fails. We see that the proposed LRCV model is much more robust than the LBF model. The numbers of iterations and CPU running time of the three models are listed in Table 3. We can see that in this experiment the proposed LRCV model converges about 10 times faster than the LBF model and about 30 times than the LCV model. Note that the LCV model fails to segment the blood vessel images in all the experiments.

Finally, in Fig. 6 we show the segmentation results on a brain MR image by the LBF model, the LCV model and the proposed LRCV model. With the same initial contours, both the LBF model and the LRCV model achieve almost the same results, but the LCV model fails. Table 4 lists the number of iterations and the required CPU time by the three models. From Table 4, we can observe that the number of iterations and the required CPU time of the LRCV model are much less than those of the LBF model and the LCV model.

To study the effect of various noise types on the performance and compare the performance between the LBF model and our proposed LRCV model, a synthetic image is added zero-mean Gaussian white noise and the salt and pepper noise, and the segmentation results are shown in Figs. 7 and 8, respectively.

Table 4
The number of iterations and CPU time by LBF, LCV and LRCV.

	The LBF model		The LCV model		The LRCV model	
	Iterations	CPU time(s)	Iterations	CPU time(s)	Iterations	CPU time(s)
Row 1	300	7.418	1000	38.324	110	2.298
Row 2	200	6.340	800	20.658	60	1.208

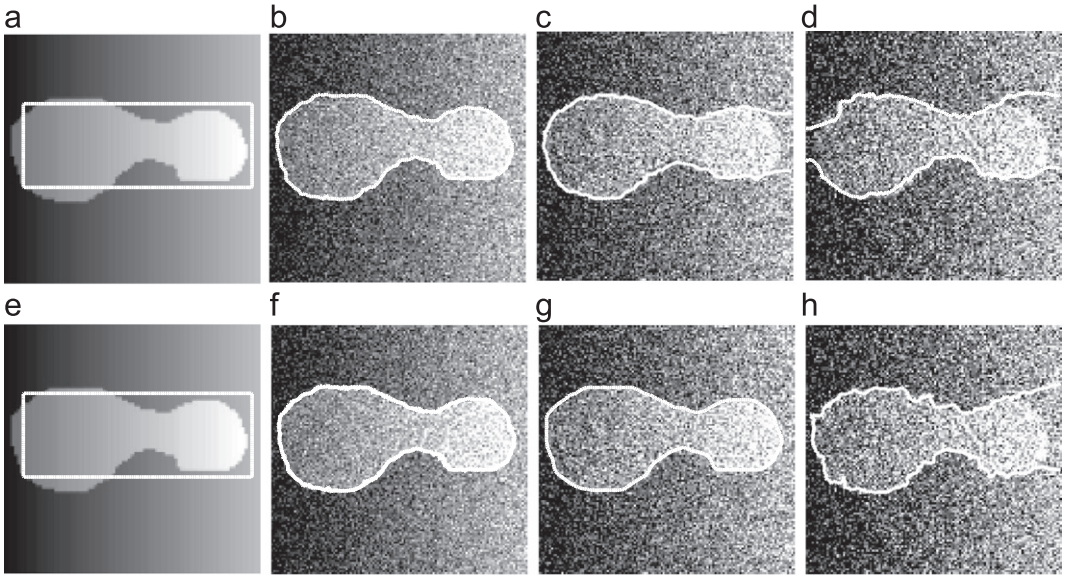

Fig. 7. Comparisons of the LBF model and the LRCV model on segmentation results with zero-mean Gaussian white noise. Row 1: by the LBF model; Row 2: by the LRCV model. Column 1: the original images and initial contours; Columns 2, 3 and 4 are added Gaussian white noise with variances 0.025, 0.05 and 0.075, respectively.

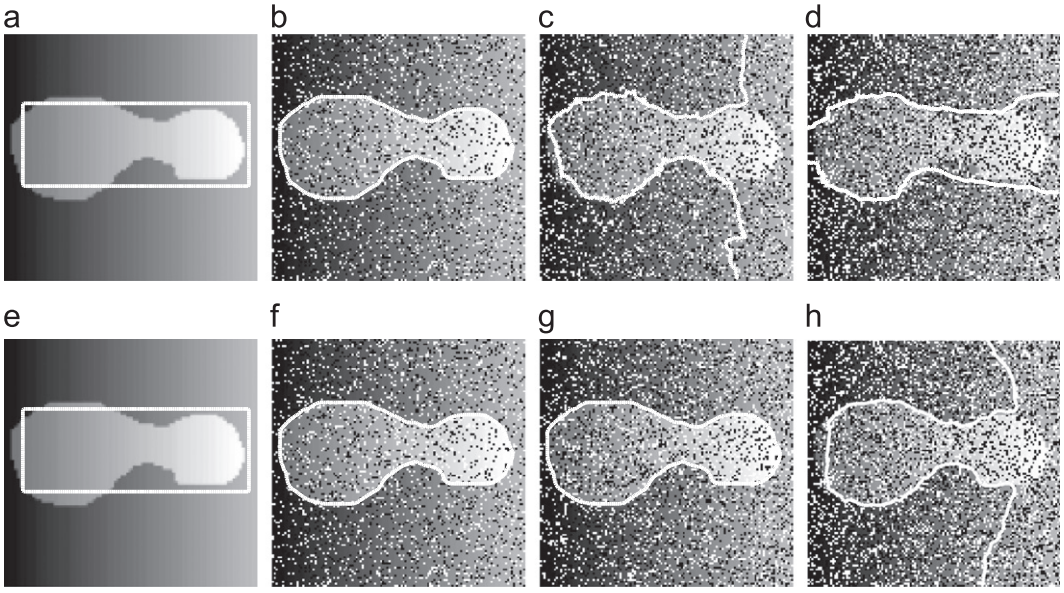

Fig. 8. Comparisons of the LBF model and the LRCV model on segmentation results with salt and pepper noise. Row 1: by the LBF model; Row 2: by the LRCV model. Column 1: the original images and initial contours; Columns 2, 3 and 4 are added the salt and pepper noise with densities 0.2, 0.3 and 0.4, respectively.

All the original images and initial contours are shown in Column 1. Columns 2, 3 and 4 in Fig. 7 show the segmentation results on image added zero-mean Gaussian white noise with variances 0.025, 0.05 and 0.075, respectively. In Fig. 8, the segmentation results on image added salt and pepper noise with densities 0.2, 0.3 and 0.4 are also shown in Columns 2, 3 and 4, respectively. Note that all the noise parameters are normalized and they correspond to operations with images with intensities ranging from 0 to 1. From Figs. 7 and 8, we can observe the proposed LRCV model has higher antinoise than the LBF model. At the same time, from the comparison between Figs. 7 and 8, we can see that both the LBF model and the proposed LRCV model have higher antinoise for the salt and pepper noise than for the Gaussian white noise.

6. Conclusion

In this paper, we proposed a new region-based active contour model, i.e., local region-based Chan–Vese (LRCV) model, for image segmentation. The LRCV model can efficiently segment the images with intensity inhomogeneity by employing the local image information. Meanwhile, for an automated initialization, a degraded CV model was proposed, whose segmentation result is taken as the initial contour of the LRCV model. Experimental results on both synthetic and real images demonstrated that the proposed LRCV model is very robust and efficient. Compared with the well-known local binary fitting (LBF) model and the LCV model, the LRCV is not only much more computationally efficient and but also much less sensitive to the initial contour.

Acknowledgments

This work is supported by the National Natural Science Foundation of China (No. 60805016), the Natural Science Foundation of Shaanxi Province of China (No. 2011JM8014), Research Fund for the Doctoral Program of Higher Education of China (No. 200807181007), the Fundamental Research Funds for the Central Universities (No. GK201002016) and China Postdoctoral Special Science Foundation (No. 200902594).

References

[1] K. Kolev, M Klodt, T. Brox, S. Esedoglu, D. Cremers, Continuous global optimization in multiview 3D reconstruction, International Journal of Computer Vision 84 (1) (2009) 80–96.
[2] M. Pollefeys, D. Nistér, J. Frahm, et al., Detailed real-time urban 3D reconstruction from video, International Journal of Computer Vision 78 (2–3) (2008) 143–167.
[3] B. Peng, L. Zhang, D. Zhang, et al., Image segmentation by iterated region merging with localized graph cuts, Pattern Recognition 44 (10–11) (2011) 2527–2538.
[4] K. Zhang, L. Zhang, S. Zhang, A variational multiphase level set approach to simultaneous segmentation and bias correction, in: Proceedings of the 17th IEEE International Conference on Image Processing, Hong Kong, 2010, pp. 4105–4108.
[5] B. Peng, L. Zhang, J. Yang, Iterated Graph Cuts for Image Segmentation, ACCV 2009.
[6] M. Kass, A. Witkin, D. Terzopoulos, Snakes: active contour models, International Journal of Computer Vision 1 (4) (1987) 321–331.
[7] C. Xu, J. Prince, Snakes, shapes, and gradient vector flow, IEEE Transactions on Image Processing 7 (3) (1998) 359–369.
[8] S. Osher, J. Sethian, Fronts propagating with curvature dependent speed: algorithms based on Hamilton–Jacobi formulation, Journal of Computational Physics 79 (1988) 12–49.
[9] V. Caselles, R. Kimmel, G. Sapiro, Geodesic active contours, International Journal of Computer Vision 22 (1) (1997) 61–79.
[10] C. Li, C. Xu, C. Gui, M. Fox, Level set evolution without re-initialization: a new variational formulation, in: Proceedings of the IEEE Conference on Computer Vision and Pattern Recognition, San Diego, 2005, pp. 430–436.
[11] K. Zhang, L. Zhang, H. Song, W. Zhou, Active contours with selective local or global segmentation: a new formulation and level set method, Image and Vision Computing 28 (4) (2010) 668–676.
[12] D. Mumford, J. Shah, Optimal approximation by piecewise smooth function and associated variational problems, Communication on Pure and Applied Mathematics 42 (1989) 577–685.
[13] J. Ning, L. Zhang, D. Zhang, C. Wu, Interactive image segmentation by maximal similarity based region merging, Pattern Recognition 43 (2) (2010) 445–456.
[14] T. Chan, L. Vese, Active contours without edges, IEEE Transaction on Image Processing 10 (2) (2001) 266–277.
[15] L. Vese, T. Chan, A multiphase level set framework for image segmentation using the. Mumford and Shah model, International Journal of Computer Vision 50 (3) (2002) 271–293.
[16] A. Tsai, A. Yezzi, A. Willsky, Curve evolution implementation of the Mumford–Shah functional for image segmentation, denoising, interpolation, and magnification, IEEE Transaction on Image Processing 10 (8) (2001) 1169–1186.
[17] R. Ronfard, Region-based strategies for active contour models, International Journal of Computer Vision 13 (2) (1994) 229–251.
[18] K. Zhang, H. Song, L. Zhang, Active contours driven by local image fitting energy, Pattern Recognition 43 (4) (2010) 1199–1206.
[19] C. Li, C. Kao, J. Gore, Z. Ding, Implicit active contours driven by local binary fitting energy, in: Proceedings of the IEEE Conference on Computer Vision and Pattern Recognition (CVPR), 2007, pp. 1–7.

[20] C. Li, C. Kao, J.C. Gore, Z. Ding, Minimization of region-scalable fitting energy for image segmentation, IEEE Transaction on Image Processing 17 (10) (2008) 1940–1949.
[21] L. Wang, C. Li, Q. Sun, D. Xia, C. Kao, Active contours driven by local and global intensity fitting energy with application to brain MR image segmentation, Journal of Computerized Medical Imaging and Graohics 33 (7) (2009) 520–531.
[22] X. Wang, D. Huang, H. Xu, An efficient local Chan–Vese model for image segmentation, Pattern Recognition 43 (3) (2010) 603–618.
[23] 〈http://www.engr.uconn.edu/~cmli/research/〉.

Shigang Liu was born in Jiangxi, China in1973. He received the B.S. and M.S. degrees from Harbin Engineering University, Harbin, China, in 1997 and 2001, respectively. In 2005, he received his Ph.D. degrees from Xidian University of China. From 2007 to 2009, he was a postdoc in the Xi'an Jiaotong University. Since 2009, he has been an Assistant Professor in the School of Computer Science, The Shaanxi Normal University. His research interests include pattern recognition and image processing.

Yali Peng was born in Shannxi, China in 1979. She got her M.S. degree from Harbin Engineering University, Harbin, China, in 2005. Since 2009, she has been a lecturer in the School of Computer Science, The Shaanxi Normal University. Her research interests include pattern recognition and image processing.